Defense Threat Reduction Agency
8725 John J. Kingman Road, MS-6201
Fort Belvoir, VA 22060-6201

DTRA-TR-14-80

TECHNICAL REPORT

Visualizing the Fundamental Physics of Rapid Earth Penetration Using Transparent Soils

Approved for public release; distribution is unlimited.

March 2015

HDTRA1-10-1-0049

Magued Iskander and
Stephan Bless

Prepared by:
Polytechnic Institute of New York University
6 MetroTech Center
Brooklyn, NY 11201

DESTRUCTION NOTICE:

Destroy this report when it is no longer needed.
Do not return to sender.

PLEASE NOTIFY THE DEFENSE THREAT REDUCTION AGENCY, ATTN: DTRIAC/ J9STT, 8725 JOHN J. KINGMAN ROAD, MS-6201, FT BELVOIR, VA 22060-6201, IF YOUR ADDRESS IS INCORRECT, IF YOU WISH THAT IT BE DELETED FROM THE DISTRIBUTION LIST, OR IF THE ADDRESSEE IS NO LONGER EMPLOYED BY YOUR ORGANIZATION.

REPORT DOCUMENTATION PAGE

Form Approved
OMB No. 0704-0188

1. REPORT DATE *(DD-MM-YYYY)*	**2. REPORT TYPE**	**3. DATES COVERED** *(From - To)*
00-03-2015	Technical	April 7, 2010 - April 7, 2014

4. TITLE AND SUBTITLE

Visualizing the Fundamental Physics of Rapid Earth Penetration Using Transparent Soils

5a. CONTRACT NUMBER
HDTRA1-10-1-0049

5b. GRANT NUMBER

5c. PROGRAM ELEMENT NUMBER

6. AUTHOR(S)

Magued Iskander
Stephan Bless

5d. PROJECT NUMBER

5e. TASK NUMBER

5f. WORK UNIT NUMBER

7. PERFORMING ORGANIZATION NAME(S) AND ADDRESS(ES)

Polytechnic Institute of New
York University
6 MetroTech Center
Brooklyn, NY 11201

8. PERFORMING ORGANIZATION REPORT NUMBER

9. SPONSORING / MONITORING AGENCY NAME(S) AND ADDRESS(ES)

Defense Threat Reduction Agency
8725 John J. Kingman Road
Fort Belvoir, VA 22060
PM/Suhithi Peiris

10. SPONSOR/MONITOR'S ACRONYM(S)
DTRA

11. SPONSOR/MONITOR'S REPORT NUMBER(S)
DTRA-TR-14-80

12. DISTRIBUTION / AVAILABILITY STATEMENT

Approved for public release; distribution is unlimited.

13. SUPPLEMENTARY NOTES

14. ABSTRACT

Many new experimental techniques were developed in the course of this effort. Measurements of the resisting stress for soil penetration have been obtained with unprecedented precision and over an unprecedented wide range of impact variables. New transparent surrogates that better mimic the high strain rate behavior of sand have been developed. New DIC analysis techniques have been developed. New ways to visualized in situ movements in sand during penetration have been devised, and have been demonstrated for static and dynamic penetration.

15. SUBJECT TERMS

sand penetration index-matching terradynamics earth penetration DIC fused quartz

16. SECURITY CLASSIFICATION OF:			**17. LIMITATION OF ABSTRACT**	**18. NUMBER OF PAGES**	**19a. NAME OF RESPONSIBLE PERSON**
a. REPORT	**b. ABSTRACT**	**c. THIS PAGE**	UU	22	Suhithi Peiris
Uclassified	Unclassified	Unclassified			**19b. TELEPHONE NUMBER** *(include area code)* 703-767-4732

CONVERSION TABLE

Conversion Factors for U.S. Customary to metric (SI) units of measurement.

MULTIPLY →	BY →	TO GET
TO GET ←	BY ←	DIVIDE
angstrom	1.000 000 x E -10	meters (m)
atmosphere (normal)	1.013 25 x E +2	kilo pascal (kPa)
bar	1.000 000 x E +2	kilo pascal (kPa)
barn	1.000 000 x E -28	meter^2 (m^2)
British thermal unit (thermochemical)	1.054 350 x E +3	joule (J)
calorie (thermochemical)	4.184 000	joule (J)
cal (thermochemical/cm^2)	4.184 000 x E -2	mega joule/m^2 (MJ/m^2)
curie	3.700 000 x E +1	*giga bacquerel (GBq)
degree (angle)	1.745 329 x E -2	radian (rad)
degree Fahrenheit	$t_k = (t^of + 459.67)/1.8$	degree kelvin (K)
electron volt	1.602 19 x E -19	joule (J)
erg	1.000 000 x E -7	joule (J)
erg/second	1.000 000 x E -7	watt (W)
foot	3.048 000 x E -1	meter (m)
foot-pound-force	1.355 818	joule (J)
gallon (U.S. liquid)	3.785 412 x E -3	meter^3 (m^3)
inch	2.540 000 x E -2	meter (m)
jerk	1.000 000 x E +9	joule (J)
joule/kilogram (J/kg) radiation dose absorbed	1.000 000	Gray (Gy)
kilotons	4.183	terajoules
kip (1000 lbf)	4.448 222 x E +3	newton (N)
kip/$inch^2$ (ksi)	6.894 757 x E +3	kilo pascal (kPa)
ktap	1.000 000 x E +2	newton-second/m^2 ($N-s/m^2$)
micron	1.000 000 x E -6	meter (m)
mil	2.540 000 x E -5	meter (m)
mile (international)	1.609 344 x E +3	meter (m)
ounce	2.834 952 x E -2	kilogram (kg)
pound-force (lbs avoirdupois)	4.448 222	newton (N)
pound-force inch	1.129 848 x E -1	newton-meter (N-m)
pound-force/inch	1.751 268 x E +2	newton/meter (N/m)
pound-force/$foot^2$	4.788 026 x E -2	kilo pascal (kPa)
pound-force/$inch^2$ (psi)	6.894 757	kilo pascal (kPa)
pound-mass (lbm avoirdupois)	4.535 924 x E -1	kilogram (kg)
pound-mass-$foot^2$ (moment of inertia)	4.214 011 x E -2	kilogram-meter^2 ($kg-m^2$)
pound-mass/$foot^3$	1.601 846 x E +1	kilogram-meter^3 (kg/m^3)
rad (radiation dose absorbed)	1.000 000 x E -2	**Gray (Gy)
roentgen	2.579 760 x E -4	coulomb/kilogram (C/kg)
shake	1.000 000 x E -8	second (s)
slug	1.459 390 x E +1	kilogram (kg)
torr (mm Hg, 0^0 C)	1.333 22 x E -1	kilo pascal (kPa)

*The bacquerel (Bq) is the SI unit of radioactivity; 1 Bq = 1 event/s.

**The Gray (GY) is the SI unit of absorbed radiation.

1. Objectives

The objective of this project is to understand the basic physics of rapid penetration into granular materials in general, and sand in particular. The primary approach is to visualize the *in situ* response of granular media by using a combination of highu speed photography and DIC (digital image correlation). A key aspect of this approach is use of transparent soil surrogates that mimic the behavior of natural sand when penetrated. Optical transparency is obtained by using transparent particles saturated by an index-matching fluid. In order to obtain quantitative physical data a number of new experimental techniques needed to be developed. New data produced as result of this project are being used to formulate improved physical models for penetration.

2. Status of Effort

The project began in June 2010, and has now been brought to a conclusion, except for a few publications that are in the process of being prepared for submission. Initially the project was carried on jointly at in the Civil Engineering Department of NYU Poly (Prof. Iskander) and at the Institute for Advanced Technology at the University of Texas at Austin (co-PI Dr. Bless). In July 2012, the IAT facilities began a phased shutdown, and Dr. Bless transferred to NYU Poly. Experiments and analysis are continuing at NYU Poly, but the experiments at IAT came to a conclusion when the laboratory shut down in December 2012.

Many new experimental techniques were developed in the course of this effort. Measurements of the resisting stress for soil penetration have been obtained with unprecedented precision and over an unprecedented wide range of impact variables. New transparent surrogates that better mimic the high strain rate behavior of sand have been developed. New DIC analysis techniques have been developed. New ways to visualized *in situ* movements in sand during penetration have been devised, and have been demonstrated for static and dynamic penetration.

This project has supported four PhD students (three of which have not yet graduated) and two masters students, both of which have received their degrees. There have been 18 publications in journals and conference proceedings, plus one book which has a 2015 publication date. There have also been four presentations at U.S. Army and U.S. Air Force Research Laboratories. In addition there 3 published Masters thesis and PhD dissertations and 3 to follow. There are also 6 journal publication in various states of progress.

3. Accomplishments

Note: Citations in this section refer to the Publications section.

3.1 New Experimental Techniques

Accomplishments on this project fall into two categories: development of new experimental techniques for study of the physics of penetration, and the data/implications that have resulted from these experiments. First we present descriptions of the new techniques.

3.1.1New Impact Facilities

Study of penetration into sand is best carried out in a vertical range, in order to accommodate the gradual increase in the strength of sand with depth. Consequently, we established vertical ranges at NYU and IAT. The NYU range can be used for velocities up to 250 m/s, and shoots a 10-mm projectile and the IAT range is capable of velocities twice that high and shoots a 14-mm projectile. Both ranges are designed to fire into dry or liquid-saturated materials, and both used compressed gas (air or helium) as the accelerating medium. Figure 1 illustrates the ranges. Both of these ranges employed air guns and breeches specifically designed for this project. The IAT facility is described in Peden et al, 2013; NYU facility is described in Cave et al, 2014. The IAT launcher is now at NYU, but it is not mounted.

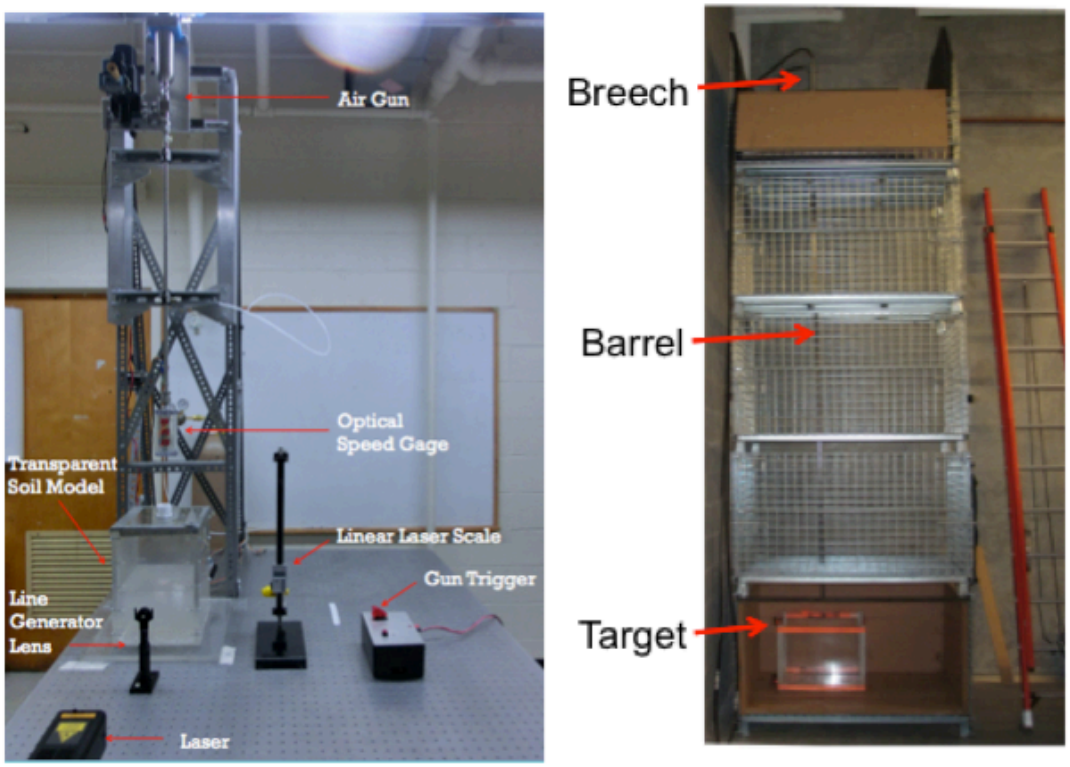

Fig. 1. Vertical impact facilities at NYU (left) and IAT (right)

3.1.2.New Measurements of Deceleration with PDV

IAT realized that its PDV probe could be used to measure deceleration in sand. In the initial proof of principle experiments a horizontal range was used, and the projectile was a .50 AP bullet. Results are shown in Figure 2 and described in Peden et al 2013.

Subsequently, a pair of PDV probes was mounted onto the muzzle of the new vertical range at IAT. It was found that the new PDV technique provided sub-m/s resolution for projectile motion. The technique was also able to observe penetration to depths exceeding 150 mm. The PDV technique was described in Peden et al 2014.

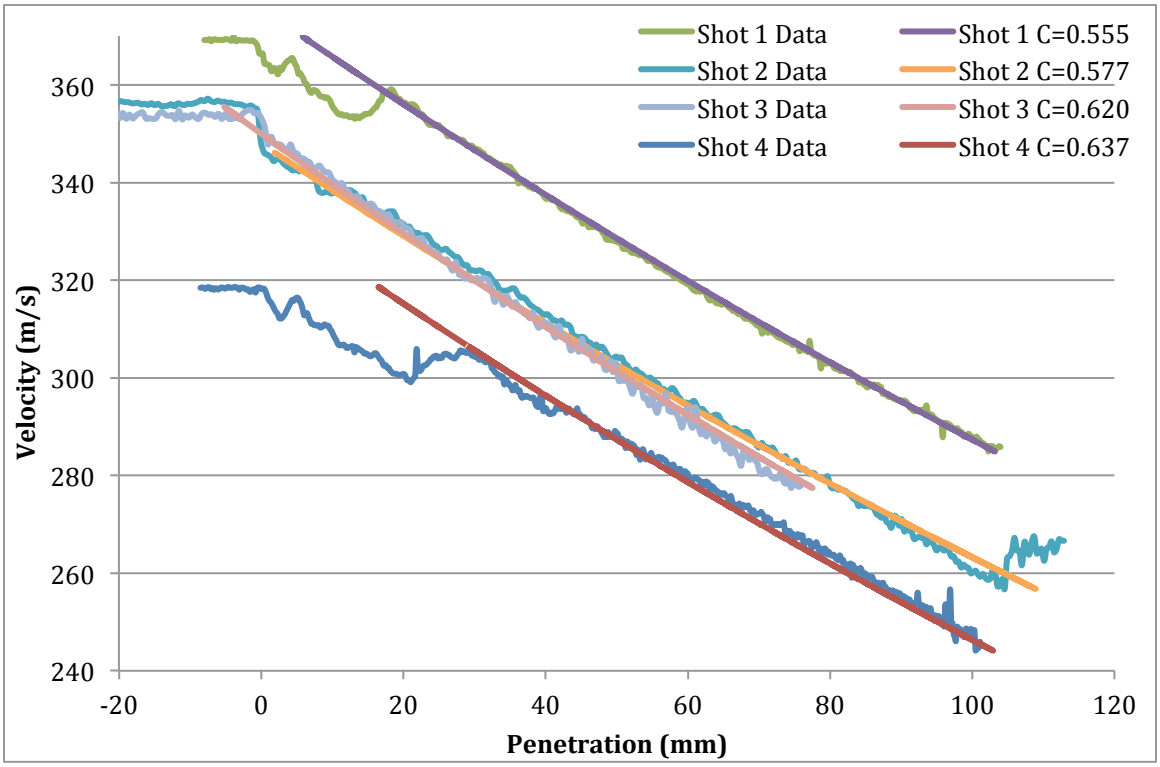

Fig. 2 Early PDV experiments, showing velocity vs time during embedment of AP bullets into sand, showing jacket stripping followed by period of constant dV/dx.

3.1.3 New Transparent Soil Surrogates

Past work with transparent soil simulants had used silica gel with an index-matched liquid. Early PDV experiments showed that the penetration resistance of that material was much less than sand. A better material was desired. The silica gel was replaced by ground fused quartz. The fused quartz was index-matched with two different liquids – a sucrose solution or a mineral oil.

Triaxial tests were performed on all these materials and behavior was a reasonable facsimile to that of natural soils. That development is described in Guzman et al, 2013, 2014a. Examples of stress-strain curves are provided in Figure 3. Along with the development of new materials, considerable effort was put into technique development to maximize transparency. It was found that most commercially-available fused quartz apparently would not wet adequately, perhaps due to small particles adhered to the grain surfaces. Pluviation rate and fluid depth were all found to be very important in obtaining optimum transparency. Discussion of new sample preparation techniques can be found in Chen et al, 2014.

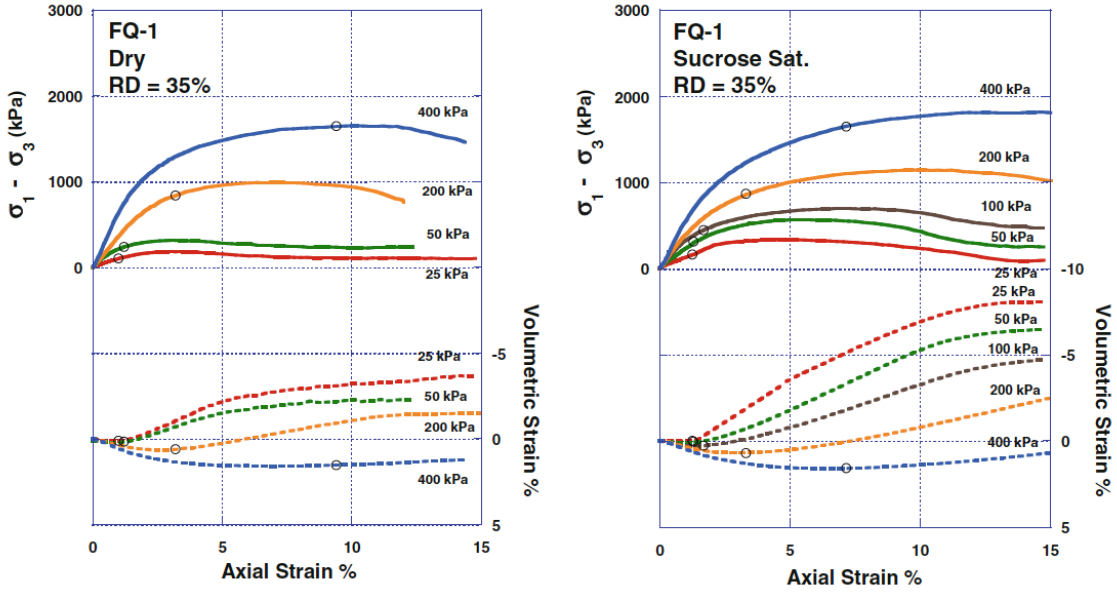

Fig. 3 Triaxial data for dry and the new sucrose-saturated fused quartz (RD=relative density).

3.1.4 Advances in high speed visualization techniques

It was realized that a higher resolution, higher framing rate high-speed camera would be necessary to resolve meso-scale motions during projectile penetration. After a thorough review of the technical requirements and evaluation of available equipment, we purchased a NAC HX5. The camera acquisition was supplemented with purchase of an optical table, special lighting and a suite of lenses suitable for taking both backlit pictures and laser illuminated pictures with our transparent soil models. It was then realized that a higher power laser and better beam-spreading optics would also be necessary, and both were acquired. A description of the new optical setup is provided in Omidvar et al. 2015a.

With the aid of the new high-speed camera, it was realized that we could now obtain displacement time information at high enough resolution and framing rate to double differentiate and obtain acceleration. This data could then be used to supplement the PDV data, which did not extend below about 50 m/s.

For this purpose long rods made from aluminum were used, with various nose shapes. Marks were added to the sides of the penetrator that were visible before complete embedment. In addition, a tail was added that would be visible above the surface of the target even after the penetrator was fully embedded. An image of one of these projectiles is shown in Fig. 4. The results of the measurements of deceleration using both the PDV and high speed photography are presented below. The experiments and results are described in Omidvar et al 2014b,c and 2015a, b.

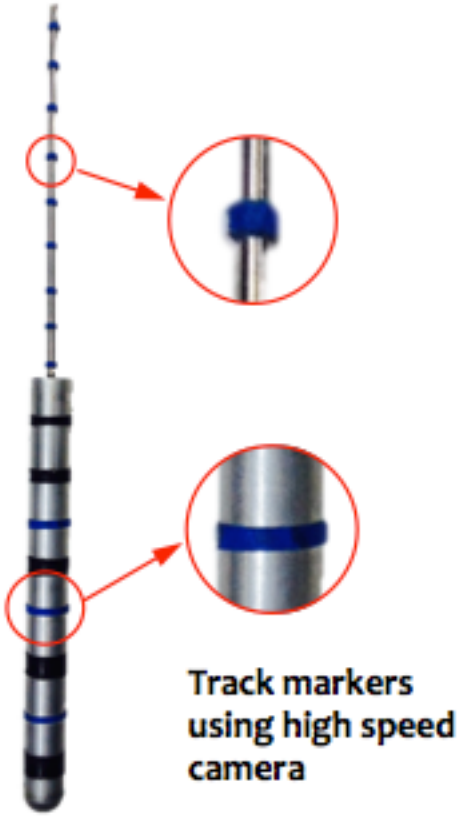

Fig. 4. Projectile designed to measure deceleration using high speed camera and opaque targets.

3.1.5 Advances in DIC techniques

There was significant progress both in DIC analysis and DIC model technology.

A new open-source program was development to carry out DIC analysis. Features were added to find the centers of grains and compute Lagrangian trajectories as well as incremental displacements. The new techniques were first applied to examine quasi-static penetration in a 2-D geometry. This allowed us to work out the

analysis technique without the complication of transparent targets. The results were remarkably well-resolved displacement fields in sand penetration. Sample results are shown in Fig. 5. The analysis method is presented in Omidvar et al. 2014d

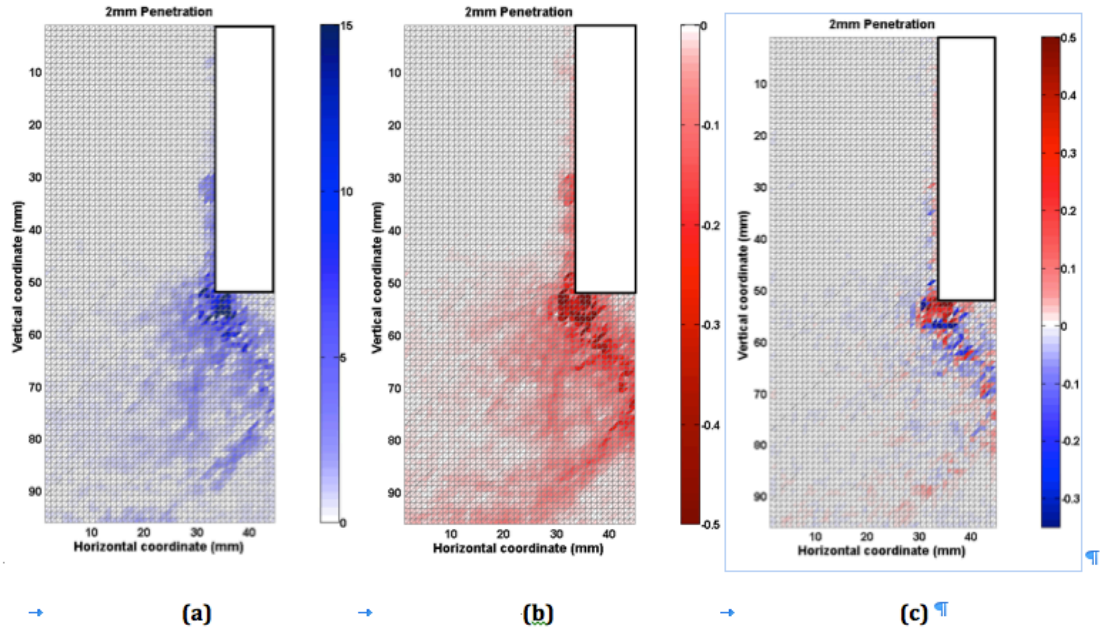

Fig. 5 Computed rotations and strains from 2mm (incremental) penetration into unconfined loose Ottawa sand (a) rigid body rotation, (b) maximum natural shear strain, and (c) volumetric strain in a 2-D quasi-static penetration, computing using new DIC analysis.

In trials it was found that the laser speckle technique that had been successful for quasi-static penetration at low penetration velocities in silica gel, presented difficulties for high speed penetration in fused quartz, because the reflection from the translucent cavity created very large gradients in illumination. In response, a completely new technique was conceived and developed. This technique involved embedding a thin layer of dyed particles in the plane of penetration within the transparent soil bed. A series of tests were conducted to determine the best areal density of particles. Images were binarized prior to DIC processing. New DIC procedures were calibrated by using digitally-displaced pairs of images. Several different DIC algorithms were evaluated, and zero-mean normalized sum of squared differences combined with multi-pass interrogation, multi-grid interrogation and subpixel estimation was identified as most appropriate for this application. New algorithms were also added to compute Lagrangian kinematics. These developments are described in Chen et al 2014, Omidvar et al 2015a.

Using this technique, we were able to obtain images during penetration that could be analyzed to yield displacement and velocity fields in the region of interest.

Figure 6 shows the disturbances in this plane created by a penetrating rod projectile, along with the displacement field in the transparent soil target.

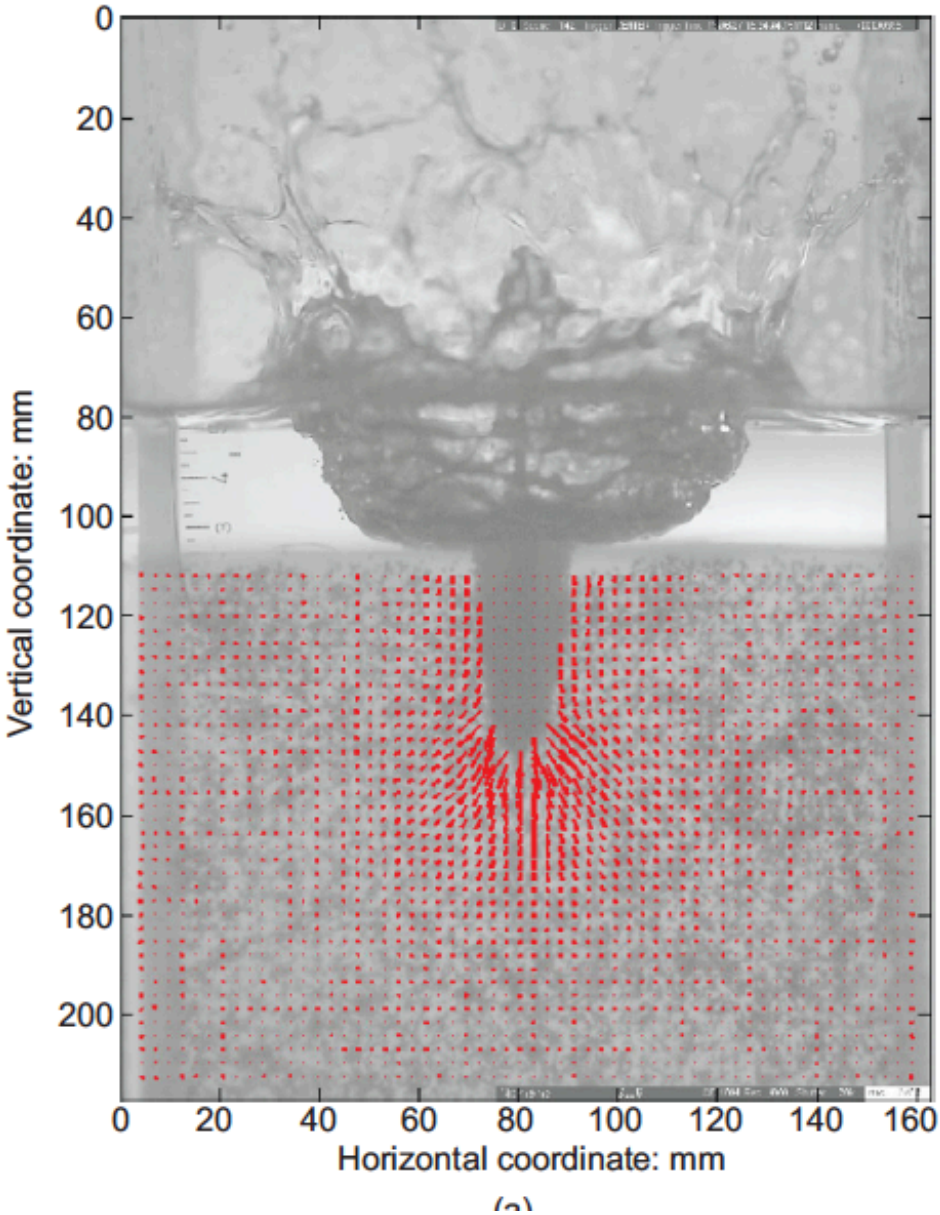

Fig. 6. Example of incremental displacement field around a conical nose 9-mm diameter aluminum projectile with an initial velocity of 14 m/s (from Chen et al, 2014)

3.2. Cavity Dynamics

Observations with the high-speed camera revealed that the penetrator is surrounded by an opaque cavity. The dynamics of this apparent cavity are

discussed in Omidvar 2015a and Guzman 2015. Examples of cavity appearance are shown in Figure 7. After analyzing numerous images as well as from experiments in which the projectile was shot along a transparent wall, it was concluded that void is created by dilation of the material around the cavity. Some of the void is then filled with air, creating a permanent opaque region around the cavity, while the outer part is filled by inward flow of pore fluid, which causes the apparent cavity to shrink in size as the penetrator comes to rest.

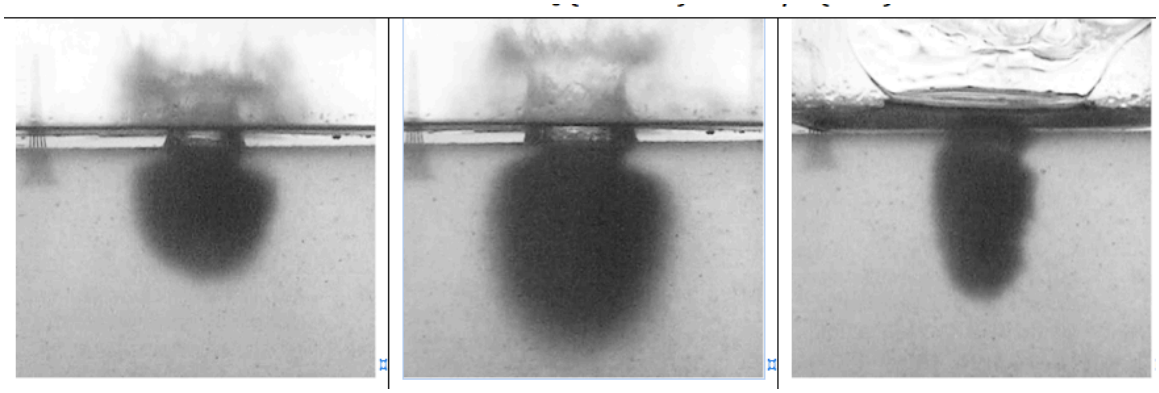

Figure 7. Apparent cavity around a penetrating the center of a sucrose-fused quartz target at 100 m/s(from Guzman et al, 2015).

3.3. Measurements of penetration resistance

In our initial work, we characterized the penetration resistance of various materials by measuring the total depth of penetration of spheres [Bless et al 2011, Guzman et al 2015].

However, the parameter of greatest interest for understanding the physics of penetration is the penetration resistance. This is a property of the target medium. It is the stress with which the target resists penetration and also the stress experienced by the penetrator. It is computed from the deceleration of the penetrator. The deceleration times the mass gives the force. The force divided by the cross section area gives the average stress.

Qualitatively, quite a lot can be learned by comparing measurements of velocity vs penetration depth for different materials. The PDV gives velocity directly. The high speed camera provides displacement times and a single differentiation gives velocity.

For the measurements of velocity histories, projectiles were either spheres or rods with hemispherical or conical shaped noses. 14 mm spheres were launched with the IAT facility, and 10-mm diameter rods L/D=10 and spheres with the NYU launcher. Spherical projectiles were made of steel, while the rods were made of

aluminum or steel; both were sufficiently hard that no projectile deformation occurred as a result of impact and penetration. Data were collected for loose and dense sand and quartz, saturated with oil or water. Impact velocities were 79 to 302 m/s.

Ideally, stress and velocity do not depend on scale for geometrically-similar objects and rate-independent materials in which gravitational forces can be neglected [Omidvar et al 2014a]. Assuming that the interaction of a penetrator with a soil mass during penetration only occurs along the nose, stress as a function of velocity should also be expected to be the same for spheres and hemispherical nosed rods. These principles can be used to combine our experiments with spheres and rods at two different diameters.

The results of these experiments are described in detail in Peden et al 2014 and Omidvar et al 2014b, 2015b. The outcome of selected tests for velocity as a function of time is shown in Fig 8. Resistance to penetration is proportional to the slopes of the $V(t)$ curves, or deceleration, as described further below. It can be seen that increasing density increases penetration resistance. At high velocities, sand has a greater penetration resistance than ground quartz, but that reverses at low velocity. It can be seen that for sand there appears to be at least two different penetration regimes, separated by a critical velocity V_c falling in the range of 70-100 m/s. The existence of the separate velocity regimes is more pronounced in dense sand compared to loose sand.

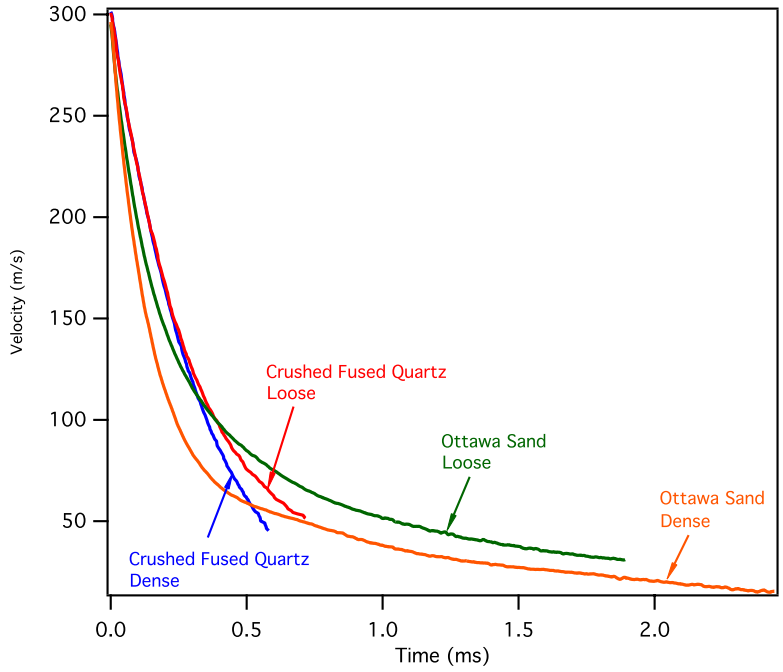

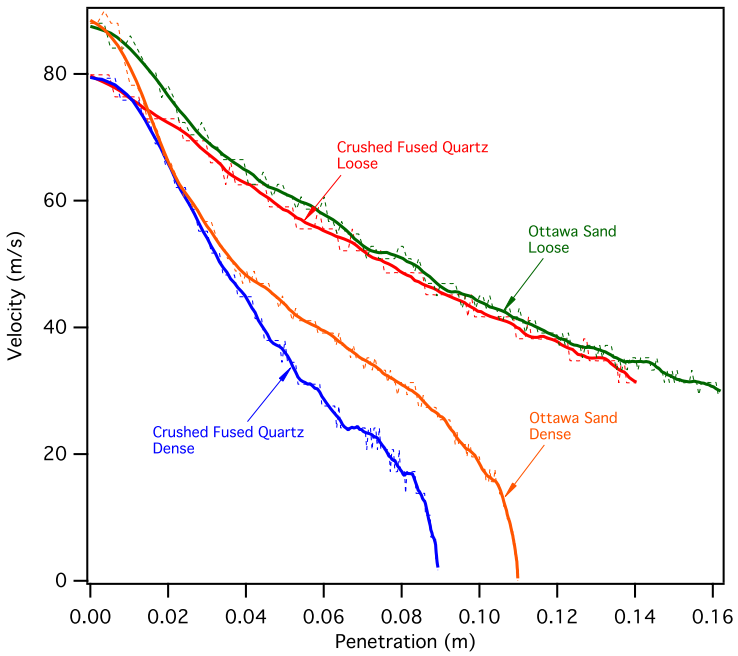

Fig 8 Data for spheres (upper) and rods (lower) penetrating Ottawa sand and crushed fused quartz (from Omidvar et al 2014b)

Further trends are discernable when the velocity data are differentiated to give acceleration. Penetration resistance (e.g. stress) as a function of velocity is plotted in Fig 9. At high velocity, the penetration resistance varies from about 130 MPa to 65 MPa, depending on the material. Interestingly, there appears to be a crossover below about 100 m/s where the penetration resistance in dense sand becomes less than fused quartz. For dense materials, there appears to be a third regime, where deceleration is nearly constant and equal to approximately 1 MPa. Note a constant deceleration leads to an infinite slope in $\mathrm{d}V/\mathrm{d}x$ as V approaches zero.

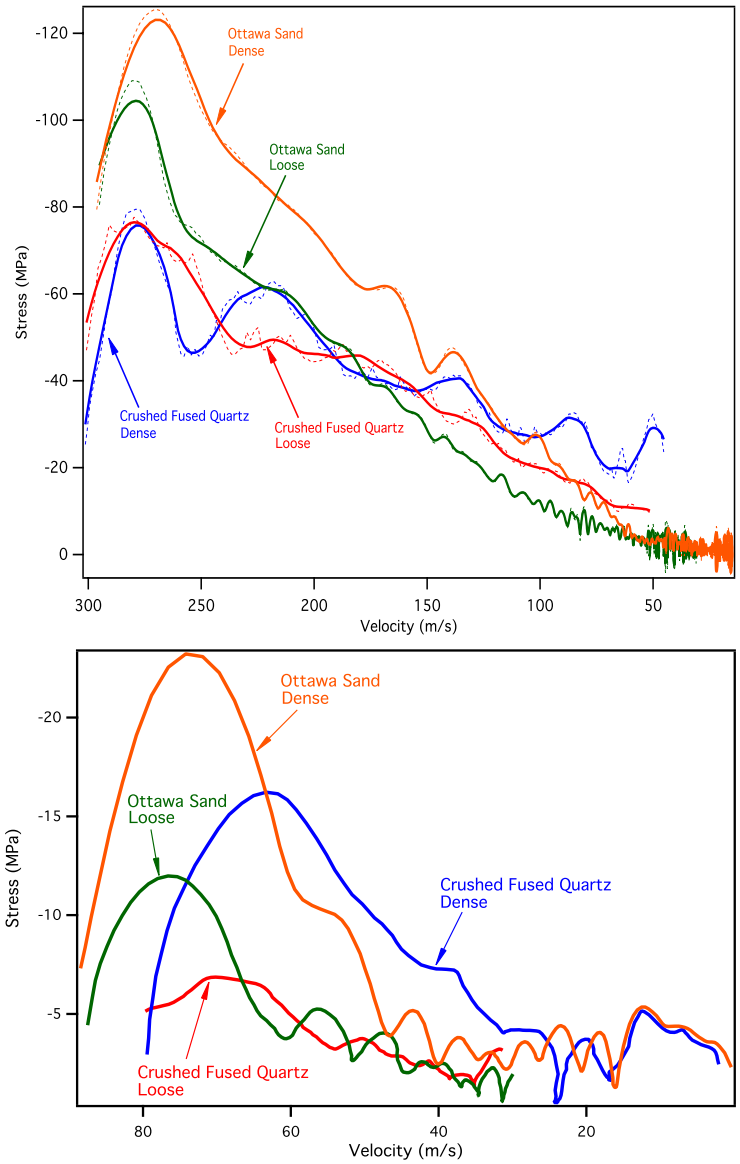

Fig 9 Penetration resistance as a function of velocity from Omidvar et al 2014b.

Penetration resistance is often considered to be a function of velocity squared. Frequently, a quadratic drag coefficient, C_D, is defined from the relationship $F=½\rho C_D A V^2$, where ρ is density. The validity of this model is checked by computing effective values of C_D. C_D is nearly constant for these materials for V>100 m/s. For dense sand, it appears to have a local maximum at about 100 m/s. The ratio of drag coefficients for loose and dry sand is also much larger than their density ratio, which suggests that C_D is not simply due to momentum transfer between the sand and the projectile. At low velocity, C_D diverges because the penetration resistance becomes almost independent of velocity, implying that $C_D \approx 1/V^2$. See Omidvar et al 2014b for more details.

To investigate the stopping force of a moving projectile, seismic earth pressure theory is being adapted to compute the stopping force. The early and necessary step was to develop a closed form method for including small amounts of cohesion into the seismic earth pressure formulation. The developed formulation is described in Iskander et al (2013a-c)

Overall, the dependence of resisting stress on velocity is consistent with a Poncelet formulation, stress = $AV^2 + R$. The first term is commonly associated with inertia, although, as pointed out in [Bless et al, 2014], frictional stresses caused by pressure also increases as V^2 increases. The Poncelet form explains why penetration resistance is proportional to V^2 at high velocities, but is nearly constant at low velocities.

It is clear from our data that there are several distinct regimes for penetration resistance in sand. Different meso-scale phenomena must dominate the penetration resistance in these regions, as discussed in Omidvar et al 2014b and Omidvar et al 2015b. Immediately after impact formation of shock waves, embedment, and stress release to the free surface all affect the deceleration. After the impact transient a steady state penetration regime occurs. For steady penetration at elevated velocities, the effective nose shape changes and the extent of material connected to force chains emanating from the projectile decreases. As the projectile is brought to rest, there is a critical velocity that depends on density below which the resistance becomes velocity independent. This suggests that a bearing stress analysis should be invoked. Indeed recent experiments on transparent soils verify the existence of a roughly hemispherical region of shear stress that is several times the diameter of a slowly penetrating projectile, as explained in the following section.

3.4. Mesoscale dynamics of penetration resistance

Fully 3D penetration was examined using the embedded plane technique coupled with the new DIC analysis procedures. An example of cumulative displacement profiles are various times is provided in Figure 10.

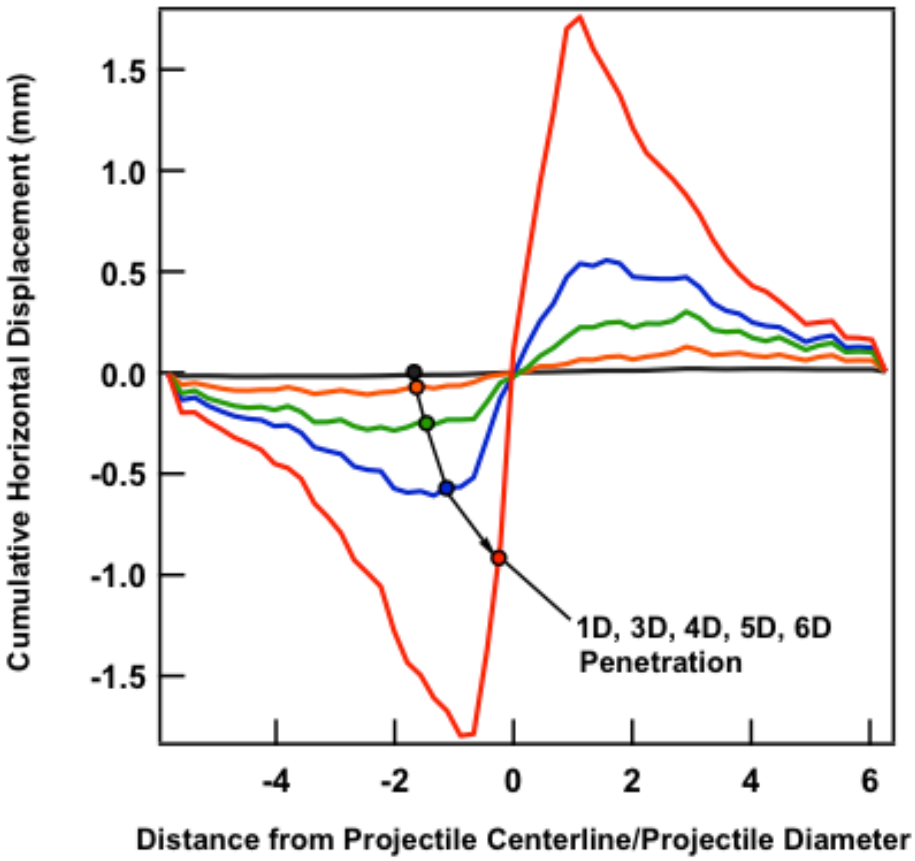

Figure 10 Cumulative horizontal displacements from 1-diameter to 6-diameters penetration, along a horizontal profile 6-diameters into the target. 9-mm rod striking at 20 m/s. From Omidvar et al 2015b.

Plots of non-affine and shear deformation have made it clear that a false nose forms in front of the penetrator. The nose has a conical shape and its form is almost independent of the original nose of the penetrator. Movement of soil around the penetrator is downward below and upward above. Modeling the displacement will require spherical cavity expansion; the simpler solutions for cylindrical cavity expansion will not be suitable. The "zone of influence" of a penetrating projectile is about six diameters.

4. Other Scholarly Activities

Two review articles were prepared on this contract. Both appeared in the International Journal of Impact Engineering and have received numerous citations (Omdivar et al 2013, 2014a). The first was concerned with high strain rate properties of sand, and the second treated high speed penetration.

A book is in preparation with the working title "Visualization of Rapid Penetration in Granular Materials." The book is edited by the co-PIs of this project. Chapters written by the editors include an introduction, a review of dynamic behavior of granular materials, a review of penetration mechanics of granular materials, and a review and results of transparent soil techniques. Other chapters have been contributed by experts in this field, including DTRA investigators John Borg, Wayne Chen, Dayakar Penumadu, Stephen Wally, Jose Andrade, Wolfgang Losert, William Proud, and John Behringer. The book will be published by Springer in 2015.

A parallel effort on the behavior of sand under uniaxial dynamic loading and triaxial high strain rate loading is underway. Early results are available in Baamer et al 2015.

A workshop was held at NYU on the mechanics of particulate materials in May 2014. It was for investigators located in the greater New York area and included participation by NYU Soft Matter Group, Yale University, New Jersey Institute of Technology, and the City College of New York. These workshops will be conducted on a semi-annual schedule.

During the course of this program seminars were presented for other DoD investigators, including the U.S. Army Research Laboratory, the U.S. Army Armaments Development and Engineering Center (ARDEC), and the Air Force Research Laboratory. There were substantive discussions for future collaborations with investigators from all of these laboratories, plus the Norwegian Defense Ministry, and we anticipate that these will lead to coordinated research activities over the next year.

5. Personnel Supported

Magued Iskander, PI, NYU Poly
Stephan Bless, Co-PI, IAT/NYU Poly
Ivan Guzman, PhD student, Civil Engineering, NYU Poly (graduated June 2014, thesis: Guzman 2014b)
Mehdi Omidvar, PhD student, Civil Engineering, NYU Poly
Bobby Peden, MS student, Engineering Mechanics, UT-Austin (graduated Dec 2012)
Zhibo Chen, PhD student, Civil Engineering, NYU Poly

Three additional students are supported at NYU Poly through the National Science Foundations Graduate STEM Fellows in K-12 Education (GK-12) program (Iskander, Co-PI). The following GK-12 fellows spend 60% of their time on this project:
Andrew Cave, MSc student, Civil Engineering, NYU Poly (graduated August 2013)
Stan Roslyakov, MSc student Civil Engineering, NYU Poly (graduated June 2014; thesis: Rosylakov 2014)
Eduardo Suescun, PhD student, Civil Engineering, NYU Poly

6. Publications

Bless, S., W.Cooper, K.Watanabe, Penetration of Rigid Rods into Sand, Int'l Symp on Ballistics, Maimi, FL, Sept 12-15, 2011

Bless, S., W.Cooper, K.Watanabi, R.Peden, Deceleration of Projectiles in Sand, Shock Compression of Condensed Matter – 2011, Chicago, Ill, June 27-July 1, 2011.

Bless S., B.Peden, I.Guzman, M.Omidvar, M.Iskander, Poncelet Coefficients of Granular Media, Dynamic Behavior of Materials Vol. 1, Chapter 45, Soc Exp Mechanics Series 2014, 373-380. Springer 2014

Baamer M. E. Suescun, N. Machairas, and M. Iskander (2015) Strain Rate Dependency of Sand Response under Uniaxial Monotonic Loading in press, GSP

Cave, A. S. Roslyakov, M.Iskander, S.Bless, Design and Performance of a Laboratory Pneumatic Gunfor Soil Ballistic Applications, DOI: 10.1111/ext.12091, Experimental Techniques, April 2014

Cave, A., Design and Performance of an Electropneumatic Gun for Visualization of Rapid Soil Penetration, M.Sc Thesis, Polytechnic Institute of New York University, May 2013

Chen, Z. M.Omidvar, M.Iskander, S.Bless, Modelling of projectile penetration using transparent soil *Int'l J. Physical Modelling in Geotechnics*, in press 2014

Chen, Z. ,M. Omidvar, M. Iskander and S.Bless (2015) Visualizing the Fundamental Physics of Rapid Earth Penetration, using Transparent Soils, in press, Geotech Sp Publ.

Guzman, I.L., M.Iskander, Geotechnical Properties of Sucrose-Saturated Fused Quartz for Use in Physical Modeling, *ASTM Geotech Testing J.,* Vol 36, No 3, doi:10.1520/GTJ20120182, 2013

Guzman, I.L., M.Iskander, E.Suescun-Florez, M.Omidvar, A transparent aqueous sand surrogate for use in physical modeling, *Acta Geotechnica* 9:187-206, DOI J0.1007/s11440-013-0247-2, 2014a

Guzman, I.L., Simulating Projectile Penetration into Granular Materials, PhD Dissertation, New York University, January 2014b

Guzman, I.J. M.Iskander, S.Bless, Terminal Depth of Penetration of Spherical Projectile in Transparent Granular Media, to appear in Granular Matter, 2015

Iskander, M*, Chen, Z., Omidvar, M., and I. Guzman (2013a) "Rankine Pseudo-Static Earth Pressure for C-f Soils," Mechanics Research Communications, Vol. 51, pp. 51-55, DOI: 10.1016/j.mechrescom.2013.04.010, Elsevier.

Iskander, M*, Chen, Z., Omidvar, M., I. Guzman and O. Elsherif (2013b) "Active Static and Seismic Earth Pressure for C-f Soils, Soils & Foundations, http://dx.doi.org/10.1016/j.sandf.2013.08.003, Vol. 53, No. 5, pp. 639 – 652, Elsevier.

Iskander, M.*, Omidvar, M., and O. Elsherif (2013c) "Conjugate Stress Approach for Rankine Seismic Earth Pressure in Cohesionless Soils," ASCE Journal of Geotechnical and Geoenvironmental Engineering, Vol. 139, No. 7, pp. 1205–1210, DOI: 10.1061/(ASCE)GT.1943-5606.0000830.

Omidvar, M., M.Iskander, S.Bless, Stress-strain behavior of sand at high strain rates, Int'l J. Impact Eng'ng 49, 192-213, 2013

M. M. Omidvar, M.Iskander, S.Bless, Response of granular media to rapid penetration, Int'l J. Impact Eng'ng, Vol 66, 60-82, 2014a

Omidvar, M., Z.Chen, S.Bless, M.Iskander, Scale Bridging Interactions During Penetration of Granular Materials, Dynamic Behavior of Materials, Vol 1, Ch 47, ed. B.Song, D.Casem, J.Kimberley, Soc Exp Mechanics, 2014b

Omidvar, M. , S.Bless., I.Guzman, M.Iskander, Velocity Regimes for Sphere Penetration in Granular Materials, Bulletin Am Phys Society, Vol 59 No 1, (abstract only) 2014c

Omdivar, Z.Chen, M.Iskander, Image Based Lagrangian Analysis of Granular Kinematics , in press, ASCE. J. Computing in Civil Engineering, 2014d

Omdivar, M., M.Iskander, S.Bless, Visualizing Kinematics of Rapid Penetration in Granular Media using Transparent Soil, in preparation, expected publication 2015a

Omdivar, M., M.Iskander, S.Bless, Deceleration Characteristics of Rapid Intrusions in Sand 2015b

Omdivar, M., Z. Chen, M.Iskander, S.Bless, Meso-Scale Kinematics of Rapid Projectile Penetration 2015c

Omdivar, M., Z. Chen, M.Iskander, S.Bless, "Evidence of Shear Induced Dilation and Particle Crushing in Rapid Penetration of Granular Media 2015d

Peden, R., S.Bless, M.Iskander, Penetration of Granular Materials: New Experimental Techniques, International Symp Ballistics, Freiburg, GE, May 2013

Peden, R., M.Omidvar S.Bless, M.Iskander, Photonic Doppler Velocimetry for Study of Rapid Penetration into Sand, Geotech Testing J., January, 2014

Roslyakov, S., Apparatus Design for isualization of Local Strain During Tri-Axial Testing using Transparent Soild, M.Sc Thesis, New York University, May 2014

Suescun, E., Review of High Strain Rate Testing of Granular Soil, in preparation, expected publication 2015.

DEPARTMENT OF DEFENSE

DEFENSE THREAT REDUCTION
AGENCY
8725 JOHN J. KINGMAN ROAD
STOP 6201
FORT BELVOIR, VA 22060
ATTN: S. PEIRIS

DEFENSE THREAT REDUCTION
AGENCY
8725 JOHN J. KINGMAN ROAD
STOP 6201
FORT BELVOIR, VA 22060
ATTN: G. DOYLE

DEFENSE TECHNICAL
INFORMATION CENTER
8725 JOHN J. KINGMAN ROAD,
SUITE 0944
FT. BELVOIR, VA 22060-6201
ATTN: DTIC/OCA

DEPARTMENT OF DEFENSE CONTRACTORS

QUANTERION SOLUTIONS, INC.
1680 TEXAS STREET, SE
KIRTLAND AFB, NM 87117-5669
ATTN: DTRIAC